BIOCHEMISTRY

 Volume 46, Number 51 December 25, 2007

Accelerated Publications

Sulfur X-ray Absorption Spectroscopy of Living Mammalian Cells: An Enabling Tool for Sulfur Metabolomics. In Situ Observation of Uptake of Taurine into MDCK Cells†

Manuel Gnida,[‡,§] Eileen Yu Sneeden,[§,||] John C. Whitin,[‡] Roger C. Prince,[⊥] Ingrid J. Pickering,[@] Małgorzata Korbas,[@] and Graham N. George*[,@]

Department of Pediatrics, Stanford University School of Medicine, 300 Pasteur Drive, Stanford, California 94305, Stanford Synchrotron Radiation Laboratory, 2575 Sand Hill Road, Menlo Park, California 94025, ExxonMobil Biomedical Sciences Inc., Annandale, New Jersey 08801, and Department of Geological Sciences, University of Saskatchewan, 114 Science Place, Saskatoon, Saskatchewan S7N 5E2, Canada

Received October 2, 2007; Revised Manuscript Received November 9, 2007

ABSTRACT: Sulfur is essential for life, with important roles in biological structure and function. However, because of a lack of suitable biophysical techniques, in situ information about sulfur biochemistry is generally difficult to obtain. Here, we present an in situ sulfur X-ray absorption spectroscopy (S-XAS) study of living cell cultures of the mammalian renal epithelial MDCK cell line. A great deal of information is retrieved from a characteristic sulfonate feature in the X-ray absorption spectrum of the cell cultures, which can be related to the amino acid taurine. We followed the time and dose dependence of uptake of taurine into MDCK cell monolayers. The corresponding uptake curves showed a typical saturation behavior with considerable levels of taurine accumulation inside the cells (as much as 40% of total cellular sulfur). We also investigated the polarity of uptake of taurine into MDCK cells, and our results confirmed that uptake in situ is predominantly a function of the basolateral cell surface.

Sulfur plays vital roles in cellular structure and function. As part of the amino acids cysteine and methionine, it is essential for protein biosynthesis, and cysteine also assists in maintaining three-dimensional protein structure through disulfide bonds. Moreover, sulfur is an important component of iron−sulfur clusters involved in redox and sulfur transfer reactions (*1*). Furthermore, sulfur-containing compounds such as glutathione (GSH),[1] a cysteine-containing tripeptide, are parts of the cellular antioxidant system (*2*, *3*). Finally, to end this selective and by far incomplete list, the sulfonic acid taurine (2-aminoethanesulfonic acid) is present in high

† This work was supported by the National Institutes of Health (R01-GM57375). Portions of this work were carried out at the Stanford Synchrotron Radiation Laboratory, which is funded by the U.S. Department of Energy, Office of Basic Energy Sciences and Office of Biological and Environmental Sciences, and the National Institutes of Health, National Center for Research Resources. Research at the University of Saskatchewan was supported in part by Canada Research Chair awards (G.N.G. and I.J.P.), the University of Saskatchewan, the Province of Saskatchewan, the Natural Sciences and Engineering Research Council of Canada, and the Canadian Institute of Health Research.

* To whom correspondence should be addressed. Telephone: (306) 966-5722. Fax: (306) 966-8593. E-mail: g.george@usask.ca.

‡ Stanford University School of Medicine.

§ These authors contributed equally to this work.

|| Stanford Synchrotron Radiation Laboratory.

⊥ ExxonMobil Biomedical Sciences Inc.

@ University of Saskatchewan.

[1] Abbreviations: GSH, glutathione; NMR, nuclear magnetic resonance; XAS, X-ray absorption spectroscopy; MDCK, Madin-Darby canine kidney; LLC-PK$_1$, Lewis lung carcinoma pig kidney; DMEM, Dulbecco's modified Eagle's medium; F-12, Ham's F-12 nutrient mixture; MEM, minimal essential medium; FBS, fetal bovine serum; PBS, phosphate-buffered saline; SSRL, Stanford Synchrotron Radiation Laboratory; PP, polypropylene; DPBS, Dulbecco's modified phosphate-buffered saline; KRPG, Krebs Ringer phosphate buffer; PC, polycarbonate.

10.1021/bi701979h CCC: $37.00
Published on Web 11/29/2007

concentrations in algae and the animal kingdom and seems to have several roles, one of the best characterized being osmoregulation (*4*). In situ measurements of the chemical speciation of sulfur in biological systems are hampered by the fact that there are only few established biophysical techniques for studying the chemical form of sulfur (*5*, *6*). ^{33}S nuclear magnetic resonance (NMR) spectroscopy, for instance, has not been widely used in examining sulfur biochemistry, although ^{33}S was among the first nuclei observed by NMR spectroscopy (*7*). The small gyromagnetic ratio, relatively large quadrupole moment, and low natural abundance combine to render ^{33}S NMR experiments uninformative and very difficult. In recent years, sulfur X-ray absorption spectroscopy (XAS) has become increasingly important in the study of sulfur species in biological systems (*8*). The X-ray absorption near-edge region of the XAS spectrum is a sensitive probe of electronic structure and hence chemical form (*9*). Near-edge spectra of sulfur compounds are particularly diverse, with a chemical shift range of ~14 eV (*5*). S-XAS has been successful as a probe of the electronic structure of sulfur-containing metalloproteins and in studying the blood biochemistry of ascidians (*10*, *11*). The technique has also been used to analyze complex mixtures by fitting experimental sulfur spectra as linear combinations of model spectra; examples include horse blood, sulfur bacteria, shiitake mushroom, horseradish, and wasabi (*5*, *12*−*14*), effectively providing an in situ measurement of all the sulfur species that are present, the sulfur metabolome. Here, we present a comprehensive S-XAS analysis of Madin-Darby canine kidney (MDCK) cell cultures, which, to our knowledge, is the first in situ observation of sulfur biochemistry in living mammalian tissue culture. MDCK cells are from a cell line that grows on semipermeable surfaces such as polycarbonate membranes and develops into a polarized monolayer, exhibiting characteristics of kidney distal tubules (*15*). In this paper, we investigate intact monolayers of polarized MDCK cells and observe taurine uptake over time, dose-dependent taurine uptake, and the polarity of taurine uptake. With regard to the polarity of taurine uptake, the MDCK and Lewis lung carcinoma pig kidney (LLC-PK$_1$) cell lines will be compared.

EXPERIMENTAL PROCEDURES

Cell Culture Methods. (1) Cell Growth. Cells were cultured using standard laboratory incubators, either in the laboratory or at the beamline, maintained at 37 °C in a humidified atmosphere of 5% CO_2 and 95% air. Growth of MDCK and LLC-PK$_1$ cell lines (American Type Culture Collection, Rockville, MD) was initiated using either DMEM/F-12 medium (with L-glutamine; Invitrogen) or minimal essential medium (MEM, with Earle's salt and L-glutamine; Invitrogen). DMEM/F-12 (polarity of taurine uptake) and MEM (time- and dose-dependent taurine uptake) media were supplemented with 10% fetal bovine serum (FBS; Hyclone) and antibiotic/antimycotic mix (Invitrogen). Cells were maintained in T-75 tissue culture flasks (Corning/Costar). For XAS experiments, confluent cell layers were subcultured by trypsinization and resuspension in DMEM/F-12 and FBS or MEM and FBS. The cells were then centrifuged (15 min, 1200 rpm, H1000B Sorvall rotor, 4 °C), and cell pellets were resuspended in serum-free MDCK medium (Sigma Chemical Co.), supplemented with 2% FBS for better cell adhesion, before being seeded onto tissue culture-treated polycarbonate membranes of Transwell inserts (0.4 μm pore size, Corning/Costar) at a density of $2-3 \times 10^5$ cells/cm^2. The growth medium was changed to serum-free MDCK medium on the following day. The membrane (or filter) of the Transwell inserts on which the cells grow is a 10 μm thick porous polycarbonate film, which has reasonable X-ray transparency in the range studied and is essentially sulfur-free. Alternative growth substrates such as mylar and polypropylene films were tested, but poor cell adhesion meant that these were difficult to handle.

(2) Taurine Uptake over Time. MDCK cells were cultured for 7 days on Transwell six-well plate inserts (24 mm diameter), with 1.5 mL of medium in the insert (apical) and 2.6 mL of medium in the plate (basolateral) compartments, and were maintained in serum-free MDCK medium. On days 1, 3, 5, and 7 as well as 14 and 3.3 h before the experiment, 15 μM taurine [Sigma, in phosphate-buffered saline (PBS; Cellgro)] was added to the apical and basolateral medium. In a control sample, the medium was kept taurine-free.

(3) Dose-Dependent Taurine Uptake. MDCK cells were kept on Transwell membranes (75 mm diameter, with 9 and 13 mL of medium in the insert and plate compartments, respectively) for 6 days using serum-free MDCK medium. Apical and basolateral media either were taurine-free or contained 1.5, 15, or 150 μM taurine, added on the first day.

(4) Polarity of Taurine Uptake. MDCK and LLC-PK$_1$ cells were plated on Transwell six-well polycarbonate membranes (24 mm diameter) and maintained for 8 days in serum-free MDCK medium. One day before the experiment, taurine (50 μM) was added to either the apical or basolateral medium. In a control experiment, apical and basolateral media were kept free of taurine. LLC-PK$_1$ cells kept under serum-free and taurine-free conditions were cultured for 10 days.

X-ray Absorption Spectroscopy. (1) Experimental Setup. Sulfur XAS spectra were recorded at beamline 6-2 of the Stanford Synchrotron Radiation Laboratory (SSRL) using a Si(111) double-crystal monochromator and a downstream harmonic rejection mirror. A detailed description of the beamline can be found at http://www-ssrl.slac.stanford.edu/beamlines/bl6-2/bl6-2.html. A scheme of the experimental end station is shown in Figure 1A. X-rays enter the setup on the right through a thin polypropylene window (PP) and pass a pair of slits, which was used to adjust the beam size to approximately 1 mm (vertical) × 8 mm (horizontal). The ion chamber I_0 measures the incident beam intensity. X-ray fluorescence I_F was measured using a Stern-Heald-Lytle fluorescent ion chamber detector, which was filled with argon. The spaces between the first and second (I_0 section) and the second and third (sample section) polypropylene windows were purged with helium to minimize absorption of the soft X-rays by air. The sample itself was mounted in air, with an air gap of 1−2 mm between the polypropylene window on the sample box and the Transwell polycarbonate membrane carrying the cells.

(2) Sample Handling and Mount. Before data collection, cell cultures on Transwell polycarbonate membranes from section A were kept in an incubator (37 °C, humidified atmosphere, 5% CO_2) at the beamline. For the XAS experiment, samples of the membrane containing the cells were cut from the polystyrene support and the apical surface of the cell monolayer was typically rinsed several times with

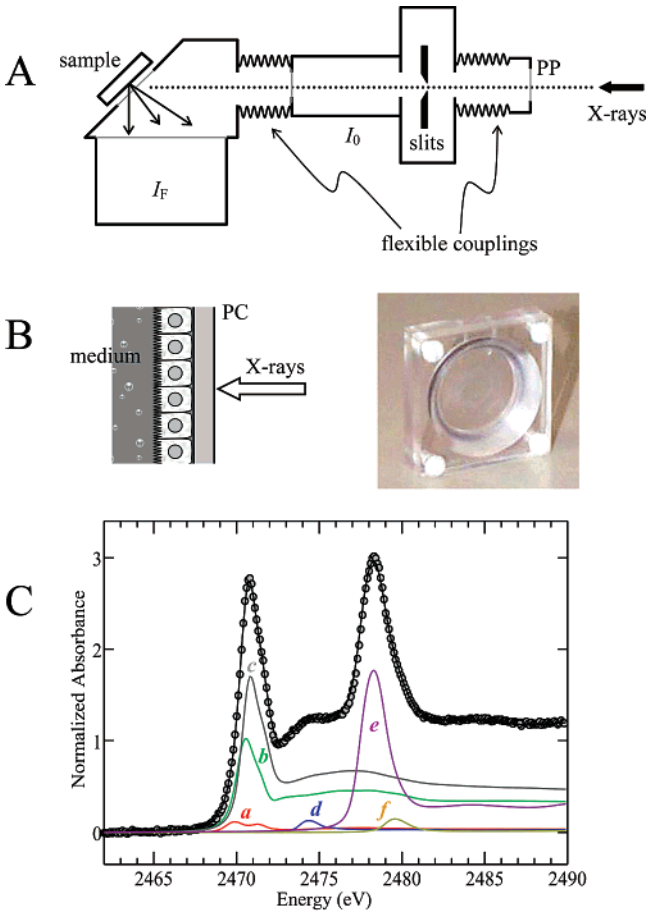

FIGURE 1: (A) Scheme of the experimental setup (viewed from the top). Abbreviations: PP, polypropylene windows (6 μm), drawn as thick gray lines; I_0, ion chamber, incident beam intensity; I_F, fluorescence detector, fluorescence intensity. The space between the first and second as well as the second and third polypropylene windows was purged with helium. The fluorescence detector was purged with argon. The sample was mounted in air. (B) Sample mount for renal epithelial cell cultures grown on polycarbonate membranes: orientation of the cell monolayer with respect to the incoming X-ray beam (left) and photograph of the sample holder (right). Abbreviation: PC, polycarbonate membrane. (C) Example of an edge fitting analysis, showing the normalized experimental near-edge spectrum as filled circles, the least-squares fit (the solid line running through the points), together with the components: (*a*) RSSR, (*b*) RSH, (*c*) RSR′, (*d*) RSO_2^-, (*e*) RSO_3^-, and (*f*) SO_4^{2-}.

buffer {Dulbecco's modified phosphate-buffered saline (DPBS) for time-dependent taurine uptake and polarity of uptake and sulfate-free Krebs Ringer phosphate buffer [KRPG; 135 mM NaCl, 5 mM KCl, 10 mM sodium phosphate buffer (pH 7.4), 5 mM glucose, 1 mM $CaCl_2$, and 1 mM $MgCl_2$] for dose-dependent taurine uptake} to remove sulfate and the S-containing dye phenol red from the growth medium. Subsequently, cells on polycarbonate membranes (PC) were mounted in the sample holder depicted in Figure 1B, with the basolateral side facing the beam. To prevent the cells from drying out during the experiment, the sample holder was filled with growth medium or buffer through filling holes (apical side of cell layer). Typically, sample holders were filled using the same buffer that was used for rinsing the cells. Under these conditions, the detection limit for sulfur concentrations is in the millimolar range, and micromolar levels of taurine (for example) present in the growth medium could not be detected. Taurine accumulates inside the cells, and the level reaches millimolar concentrations; therefore, XAS spectra with good signal-to-noise ratios were produced.

(3) Data Collection and Processing. XAS data were collected in the energy range of 2450−2600 eV using the XAS Collect software (*16*), using a count time of 0.2 s per point, with approximately 7 min per energy scan, with the structured region being acquired in the first 2 min. Two sweeps were generally taken per sample to check for reproducibility. X-ray-induced damage is an issue that has to be considered. When multiple spectra were taken at identical sample positions, changes in the spectra were observed to accumulate (see the Supporting Information), indicating progressive damage to the sample caused by the beam. Conversely, when the sample was translated to a new (unexposed) position between sweeps, the spectra were observed to be essentially identical (*17*). The diameter of the sample holder allowed for a maximum of five beam spot positions, and repeat spectra were routinely recorded at a minimum of two locations. Energy calibration was performed by reference to the K-edge spectrum of a freshly prepared sodium thiosulfate standard recorded frequently during the experiments, assuming the lowest energy peak to be at 2469.2 eV (*18*). Data processing, including background removal and normalization (see the Supporting Information), was performed using the EXAFSPAK suite of programs (G. N. George, Stanford Synchrotron Radiation Laboratory) and PySpline (A. Tenderholt, Stanford University).

(4) Edge Fits. The S-XAS spectrum of cell cultures represents a mixture of several sulfur species (the cellular sulfur metabolome). Using DATFIT from the EXAFSPAK program package, spectra were deconvoluted by least-squares fitting a linear combination of reference compound spectra to the data (*5*). This process is illustrated in Figure 1C which shows a spectrum of MDCK cells with the components used to fit the spectrum superimposed. We note that the dilute nature of the spectra from the cell cultures means that a systematic error due to baseline artifacts affects the estimate of the edge jump, and that this results in totals that differ from 100%. Renormalization of the fraction of each component obtained by least-squares using the total estimated from the fitting will provide superior estimates of total sulfur because the sharp features of the near-edge spectra will be relatively unaffected by baseline problems and the spectra of model compound solutions, which are more concentrated, do not suffer from normalization errors due to poor baseline. The data in Tables 1 and 2 and in Figure 2 were renormalized to the total obtained in the curve fitting. Higher derivatives of the spectra and fits were inspected to ensure adequate fitting to regions where overlapping peaks were present (see the Supporting Information). Model compounds (spectra of aqueous solutions at or near pH 7, except as noted below) used in the fits were oxidized glutathione (*a*, RSSR), reduced glutathione (*b*, RSH), methionine (*c*, RSR′), methionine sulfoxide (not significant in Figure 1C, RR′SO), cysteine-sulfinic acid (pH 8.5) (*d*, RSO_2^-), taurine (*e*, RSO_3^-), and sulfate (pH 8.2) (*f*, SO_4^{2-}). We note in passing that the specific compounds are representatives of sulfur functional groups and are not explicitly identified by this method (*5*). For example, the spectra of oxidized glutathione and other biological disulfides are essentially indistinguishable (not illustrated), and oxidized glutathione is therefore used to

Table 1: Cellular Sulfur Content Determined by Fitting a Linear Combination of Models to the Spectra Shown in Figure 2[a]

(A)

days in taurine	RSSR	RSH	RSR′	RR′SO	RSO_2^-	RSO_3^-	SO_4^{2-}	N_{tot}	residual
0	4.6(5)	38.8(13)	51.1(9)	1.4(3)	2.2(2)	1.3(2)	0.9(1)	109	0.8
0.14	8.0(4)	36.0(9)	46.7(6)	1.2(2)	1.8(2)	6.1(1)	0.5(1)	109	0.4
0.58	2.5(5)	38.9(12)	45.9(9)	1.1(2)	2.1(2)	9.2(2)	0.8(1)	107	0.7
1	3.9(4)	33.9(11)	48.0(8)	1.1(2)	1.8(2)	10.8(2)	0.8(1)	112	0.5
3	2.3(4)	37.0(11)	46.9(7)	1.2(2)	2.2(2)	10.1(2)	0.7(1)	112	0.5
5	2.1(5)	34.6(13)	44.0(9)	0.6(3)	1.2(2)	17.1(2)	0.7(1)	111	0.7
7	2.8(5)	29.2(12)	43.6(8)	1.2(2)	1.7(2)	21.0(2)	1.0(1)	108	0.6

(B)

[taurine] (μM)	RSSR	RSH	RSR′	RR′SO	RSO_2^-	RSO_3^-	SO_4^{2-}	N_{tot}	residual
0	14.8(7)	27.1(18)	48.6(13)	4.5(3)	0.9(3)	4.1(2)	0.4(1)	111	1.6
1.5	20.4(10)	24.2(26)	43.0(18)	8.2(5)	0.8(4)	3.6(3)	–	108	3.3
15	14.5(8)	16.2(21)	37.4(14)	3.8(4)	0.9(4)	26.1(3)	1.4(2)	110	2.0
150	8.4(8)	15.4(21)	32.7(14)	2.3(4)	0.5(4)	40.3(3)	0.6(2)	103	2.1

[a] Fit values are given in percent except the dimensionless fit residual. Values in parentheses represent the precision of the last digit derived from the fit (estimated standard deviations obtained from the diagonal elements of the covariance matrix). Residual values are a measure for the goodness of the fit and depend on the noise level. All values have been renormalized using N_{tot}, the total sulfur, which should be close to 100%; deviations from 100% arise primarily from normalization errors (as discussed in the text). A description of edge fitting can be found elsewhere (*12*).

Table 2: Edge Fit Parameters Corresponding to Spectra Shown in Figure 3[a]

(A)

MDCK	RSSR	RSH	RSR′	RR′SO	RSO_2^-	RSO_3^-	SO_4^{2-}	N_{tot}	residual × 10^3
no taurine 1	4.4(5)	38.1(12)	54.8(8)	1.2(2)	1.3(2)	–	0.4(1)	108	0.6
no taurine 2	8.9(5)	33.2(11)	49.6(8)	4.1(2)	1.1(2)	2.7(2)	0.8(1)	107	0.6
apical 1	10.3(4)	23.5(11)	54.6(7)	4.9(2)	0.5(2)	5.6(1)	1.0(1)	111	0.5
apical 2	8.3(4)	33.2(11)	47.3(7)	4.1(2)	1.0(2)	5.7(1)	0.8(1)	109	0.5
basolateral 1	8.2(5)	27.0(12)	45.8(8)	2.9(2)	0.9(2)	14.4(2)	1.1(1)	112	0.6
basolateral 2	7.4(4)	31.7(10)	45.1(7)	3.6(2)	0.7(2)	11.2(1)	0.6(1)	105	0.5

(B)

LLC-PK_1	RSSR	RSH	RSR′	RR′SO	RSO_2^-	RSO_3^-	SO_4^{2-}	N_{tot}	residual × 10^3
no taurine	8.6(5)	46.8(12)	41.9(1)	2.3(2)	0.5(2)	–	0.2(1)	108	0.6
apical	13.5(4)	29.1(11)	48.6(8)	3.0(2)	0.7(2)	5.1(2)	0.9(1)	114	0.6
basolateral	14.0(7)	27.0(18)	48.6(12)	3.2(3)	–	6.7(2)	0.8(1)	112	1.5

[a] See information for Table 1. Experiments for MDCK cells were repeated once on a second polycarbonate membrane (trials 1 and 2).

determine total disulfides (RSSR), which would include protein disulfides, mixed disulfides, and oxidized gluthathione. Likewise, the use of methionine as a model does not imply measurement of free methionine, but instead of all sulfur coordinated as thioether. Perhaps the only individual metabolite that can be specifically identified is taurine (2-aminoethanesulfonate), due to the fact that it is the only biological sulfonate expected to be present.

RESULTS AND DISCUSSION

Taurine Uptake over Time. We first studied taurine uptake over time in MDCK cells that were seeded at a high density on polycarbonate membranes of Transwell inserts on day 1 and were maintained in serum-free medium for 7 days. On different days of this week, 15 μM taurine was added to the apical and basolateral media, and spectra were recorded on day 7. Figure 2A displays the corresponding normalized S-XAS spectra. By deconvolution, seven components were found to contribute significantly to the experimental cell culture signal: disulfides RSSR, thiols RSH, thioethers RSR′, sulfoxides RR′S═O, sulfinic acids RSO_2^-, sulfonates RSO_3^-, and sulfates SO_4^{2-} (Table 1A; compare also Figure 1C). The first (and largest) maximum of the spectrum at 2471 eV can be deconvoluted as containing disulfides, thiols, and thioethers, with the major representatives being protein disulfides and thiols, oxidized and reduced glutathione, and methionine. The second major peak of the X-ray absorption near-edge signal at 2478 eV is consistent with sulfonates. Taurine is by far the most abundant compound of this chemical species in mammalian biology (*4*).

It is evident from Figure 2A (top and bottom panels) and the fit results in Table 1A that the sulfonate/taurine content in the cells correlates with the length of time taurine was present in the growth medium. Cellular taurine percentages increase quickly from negligible amounts to more than 10% within the first 24 h and reach a saturation level of more than 20% when taurine is present for 7 days. This trend in taurine uptake behavior has been confirmed in a replicate experiment (data not shown).

While the taurine fraction of total cellular sulfur increased from 1% (0 days) to 21% (7 days), the respective value for the combined RSSR/RSH/RSR′ fraction dropped by 19%. This reciprocal behavior could indicate either taurine production or taurine uptake. In the first case, an increasing amount of taurine would be balanced by a reduction of the signal intensities of its precursors. In the second case, increasing amounts of cellular taurine due to uptake would result in a decreasing contribution of the RSSR/RSH/RSR′ fraction

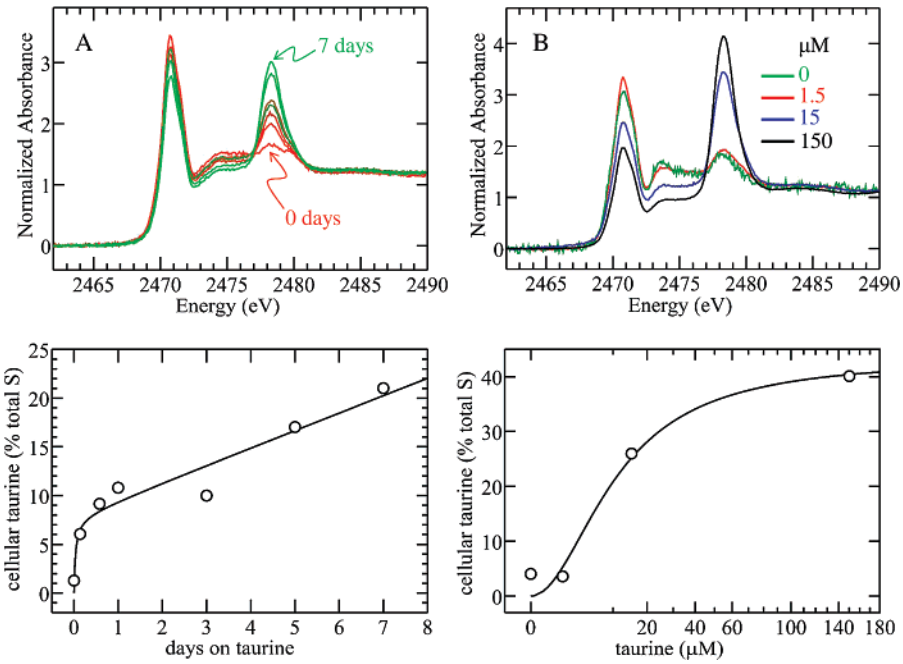

FIGURE 2: (A) Uptake of taurine over time by serum-free MDCK cells supplemented with 15 μM taurine for the indicated times. All cultures were 7 days old on the day of the XAS experiment. (B) Dose dependence of uptake of taurine into MDCK cells. The bottom panels display the (A) time and (B) dose dependence of cellular sulfonate/taurine levels. Parameters of corresponding edge fits are listed in Table 1.

since our normalization procedure sets the absorption edge jump to 1 (100% total sulfur). An important observation is that taurine levels in cultured MDCK cells depend only on the availability of medium taurine since little taurine is synthesized in cells that were kept under taurine-free conditions (0 days of taurine in culture, 1% cellular taurine). Also, the RSH/RSSR (8 → 11) and RSR′/RSH (1.3 → 1.5) ratios stay constant (0 days → 7 days), further arguing against taurine synthesis. Indeed, normalizing the absorption edges of the whole series to the first maximum demonstrates that the only spectral changes observed are an increase in taurine peak intensity and a related increase in the edge jump (data not shown). The increases in edge jump for the different time points with respect to $t = 0$ days are in excellent agreement with the values for the cellular taurine levels given in Table 1A. We therefore conclude that the reciprocal behavior of taurine and the RSSR/RSH/RSR′ fraction results from our normalization procedure and reflects exclusively uptake of taurine by the cells and not taurine synthesis.

Dose-Dependent Taurine Uptake. In addition to time dependence, we observed dose dependence of uptake of taurine into MDCK cells (Figure 2B and Table 1B). Cells were kept for 6 days in serum-free medium that contained different amounts of taurine. Clearly, the peak height and taurine fraction of sulfur in the cells were correlated with the amount of taurine present during culture. In the range of 1.5−150 μM, the dose dependence shows saturation of uptake at large doses (Figure 2B, bottom panel). It also should be noted that taurine can accumulate at very high levels in MDCK cells: a concentration of 150 μM taurine in the growth medium results in cells in which ∼40% of all cellular sulfur consists of taurine. Taurine transport in mammalian cells by the transporter TauT has been recently studied in detail and has been reviewed (*19*, *20*). It is known that mammalian cells are able to take up taurine against a large concentration gradient. In the myocardium, for example, accumulation of taurine can result in cellular concentrations as high as 30 mM, which is to be compared to the plasma concentration of 40−100 μM (*21*).

A comparison of the data for dose- and time-dependent taurine uptake suggests a certain variability of cellular sulfur contents for different batches of MDCK cells. The RSH/RSSR ratio was ∼10 in the time-dependent uptake experiment (Table 1A, 7 days), whereas it was ∼1 in the dose-dependent study (Table 1B, 15 μM). However, the sum of the thiol and disulfide components accounts for ∼35% of the total sulfur in both cases. This implies that the cellular environment of MDCK cells used for the dose-dependent study was more oxidized than for the time-dependent experiment. Values for the RSR′/RR′SO couple are in agreement with this argument since the thioether fraction is somewhat smaller and the sulfoxide fraction somewhat larger in the dose-dependent as compared to the time-dependent data.

Polarity of Taurine Uptake. Taurine uptake in polarized epithelia has been found to be polar (*22*). MDCK and LLC-PK_1 cells originate from different parts of the kidney tubule (MDCK from distal, LLC-PK1 from proximal), and taurine transport is thus expected to differ in that proximal cells should reabsorb filtered taurine while distal cells need to regulate cell volume in response to osmotic stress and use taurine for this purpose. Transport in MDCK cells occurs predominantly at the basolateral surface, and taurine is directed into the cell. In contrast, LLC-PK_1 cells take up taurine mainly on the apical surface, and there is a transepithelial movement of taurine from the apical to the basolateral side. The activity of the taurine transporter is regulated by external taurine concentration and osmolality (*23*, *24*). Compared to cells in standard medium (50 μM taurine), incubation of epithelial cell monolayers in taurine-free medium leads to an increase in the rate of taurine uptake, whereas exposure to high taurine levels in the medium (500

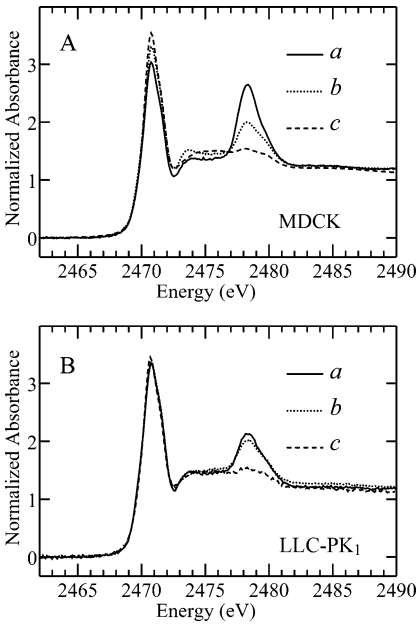

FIGURE 3: (A) Polarity of uptake of taurine into MDCK cells. (B) Uptake of taurine into LLC-PK_1 cells. Taurine (15 μM, 1 day) was added to the apical (a) or basolateral medium (b) or not added (c). Corresponding edge fits are listed in Table 2.

μM) results in a reduction in the rate of uptake. This adaptive response is due to altered rates of taurine uptake (V_{max}) rather than changes in the affinities (K_m) on both surfaces of MDCK and LLC-PK_1 cells (*20*, *24*). Taurine uptake is also enhanced in MDCK but not LLC-PK_1 cells by increasing the medium osmolality, a response that occurs mainly located at the basolateral surface (*20*, *23*, *24*). Conversely, MDCK cells that are switched back from hyperosmolar to isotonic medium (from 500 to 300 mosmol/kg) release taurine on the basolateral side to minimize cell swelling (*23*). Taurine uptake and release studies in the past have typically been performed with radioactive tracer methods using [^{3}H]- and [^{14}C]taurine (*20*, *24*). To measure tracer counts, cells grown on tissue culture-treated polycarbonate membranes have to be solubilized, thereby destroying the polarized epithelial monolayer that had previously formed. Also, from the measurement of radiolabel alone, one cannot be sure of the direction of mass transfer.

We studied the polarity of uptake of taurine into MDCK and LLC-PK_1 cells that had been maintained for 8 days in serum-free medium. On day 7, 1 day before the experiment, 50 μM taurine was added to either the apical or the basolateral medium. Taurine is taken up on both surfaces of MDCK monolayers but more by the basolateral surface (Figure 3A and Table 2A). After 1 day of exposure, sulfonate constitutes ~14% of cellular sulfur when taurine is added to the basolateral medium, but only 6% when taurine was present in the apical medium (average values of two independent measurements on different polycarbonate membranes). In contrast, the fractional taurine signals in LLC-PK_1 cells are comparable whether taurine is present in the basolateral or apical medium. We determined sulfonate percentages of 8 and 6%, respectively, after 1 day of culture in taurine-containing medium (Figure 3B and Table 2B). Accumulation levels in LLC-PK_1 cells correspond to levels reached in MDCK cells via apical uptake. It is clear from these data that MDCK cells are able to accumulate much larger amounts of taurine, an ability that is primarily mediated by taurine transport on the basolateral surface.

Our observation of the polarity of taurine uptake agrees well with previous studies using radioactive tracer methods (*22*). The rate of transport of taurine into the MCDK cell line was found to be greatest at the basolateral surface and was shown to be directed into the cell, thereby leading to accumulation of taurine inside the cells. In LLC-PK_1 cells, the rate of taurine transport was reported to be greater at the apical than the basolateral surface. However, unlike for MDCK cells, we do not observe any significant differences in cellular sulfonate content, independent of the presence of taurine in the apical or basolateral medium. On the time scale of our experiment, the reported greater rate of apical transport does not lead to a greater accumulation of taurine. A likely explanation is the transepithelial movement of taurine from the apical to the basolateral medium in LLC-PK_1 cells, which is not observed in the MDCK cell line (*22*).

CONCLUSION

We have successfully employed S-XAS to study different aspects of sulfur biochemistry in cultures of the renal epithelial MDCK and LLC-PK_1 cell lines. We show that in situ MDCK cells take up taurine in a dose- and time-dependent manner and that MDCK cells are able to accumulate much larger amounts of taurine than LLC-PK_1, an ability that is primarily mediated by taurine transport on the basolateral surface. This behavior is consistent with the different tissue origins of these two cell lines. Our results demonstrate that S-XAS is a valuable and potentially nondestructive tool for studying the sulfur metabolome of intact, living mammalian tissue.

SUPPORTING INFORMATION AVAILABLE

Figures showing background subtraction (Figure S1), effects of extensive exposure to the X-ray beam (radiation damage) upon the near-edge spectra (Figure S2), reproducibility of near-edge spectra from different locations on the layer of cultured cells (Figure S3), and higher derivatives of least-squares fitted spectra (Figure S4). This material is available free of charge via the Internet at http://pubs.acs.org.

REFERENCES

1. Beinert, H. (2000) A tribute to sulfur, *Eur. J. Biochem. 267*, 5657−5664.
2. Atmaca, G. (2004) Antioxidant effects of sulfur-containing amino acids, *Yonsei Med. J. 45*, 776−788.
3. Schafer, F. Q., and Buettner, G. R. (2001) Redox environment of the cell as viewed through the redox state of the glutathione disulfide/glutathione couple, *Free Radical Biol. Med. 30*, 1191−1212.
4. Huxtable, R. J. (1992) Physiological actions of taurine, *Physiol. Rev. 72*, 101−163.
5. Pickering, I. J., Prince, R. C., Divers, T., and George, G. N. (1998) Sulfur K-edge X-ray absorption spectroscopy for determining the chemical speciation of sulfur in biological systems, *FEBS Lett. 441*, 11−14.
6. Rompel, A., Cinco, R. M., Latimer, M. J., McDermott, A. E., Guiles, R. D., Quintanlha, A., Krauss, R. M., Sauer, K., Yachandra, V. K., and Klein, M. P. (1998) Sulfur K-Edge X-ray Absorption Spectroscopy: A Spectroscopic Tool to Examine the Redox State of S-Containing Metabolites in vivo, *Proc. Natl. Acad. Sci. U.S.A. 95*, 6122−6127.
7. Wagler, T. A., Daunch, W. A., Rinaldi, P. L., and Palmer, A. R. (2003) Solid state ^{33}S NMR of inorganic sulfides, *J. Magn. Reson. 161*, 191−197.

8. Akabayov, B., Doonan, C. J., Pickering, I. J., George, G. N., and Sagi, I. (2005) Using softer X-ray absorption spectroscopy to probe biological systems, *J. Synchrotron Radiat. 12*, 392−401.
9. George, G. N., Hedman, B., and Hodgson, K. O. (1998) An edge with XAS, *Nat. Struct. Biol. 5*, 645−647.
10. Solomon, E. I., Hedman, B., Hodgson, K. O., Dey, A., and Szilagyi, R. K. (2005) Ligand K-edge X-ray absorption spectroscopy: Covalency of ligand-metal bonds, *Coord. Chem. Rev. 249*, 97−129.
11. Frank, P., Hedman, B., and Hodgson, K. O. (1999) Sulfur allocation and vanadium-sulfate interactions in whole blood cells from the tunicate *Ascidia ceratodes*, investigated using X-ray absorption spectroscopy, *Inorg. Chem. 38*, 260−270.
12. Pickering, I. J., George, G. N., Yu, E. Y., Brune, D. C., Tuschak, C., Overmann, J., Beatty, J. T., and Prince, R. C. (2001) Analysis of sulfur biochemistry of sulfur bacteria using X-ray absorption spectroscopy, *Biochemistry 40*, 8138−8145.
13. Yu Sneeden, E., Harris, H. H., Pickering, I. J., Prince, R. C., Johnson, S., Ki, X., Block, E., and George, G. N. (2004) The sulfur chemistry of shiitake mushroom, *J. Am. Chem. Soc. 126*, 458−459.
14. Yu, E. Y., Pickering, I. J., George, G. N., and Prince, R. C. (2001) In situ observation of the generation of isothiocyanates from sinigrin in horseradish and wasabi, *Biochim. Biophys. Acta 1527*, 156−160.
15. Rindler, M. J., Chuman, L. M., Shaffer, L., and Saier, M. H. (1979) Retention of differentiated properties in an established dog kidney epithelial cell line (MDCK), *J. Cell Biol. 81*, 635−648.
16. George, M. J. (2000) XAS-Collect: A computer program for X-ray absorption spectroscopic data acquisition, *J. Synchrotron Radiat. 7*, 283−286.
17. As with any measurement made upon living systems, we cannot absolutely rule out the possibility that by the time the first measurement was made the sample was perturbed, although because of the short time taken we consider this possibility unlikely.
18. Sekiyama, H., Kosugi, N., Kuroda, H., and Ohta, T. (1986) Sulfur K-edge absorption spectra of Na_2SO_4, Na_2SO_3, and $Na_2S_2O_x$ (x=5−8), *Bull. Chem. Soc. Jpn. 59*, 575−579.
19. Lambert, I. H. (2004) Regulation of the cellular content of the organic osmolyte taurine in mammalian cells, *Neurochem. Res. 29*, 27−63.
20. Han, X., Patters, A. B., Jones, D. P., Zelikovic, I., and Chesney, R. W. (2006) The taurine transporter: Mechanisms of regulation, *Acta Physiol. 187*, 61−73.
21. Chesney, R. W., Lippincott, S., Gusowski, N., Padilla, M., and Zelikovic, I. (1986) Studies on renal adaptation to altered dietary amino acid intake: Tissue taurine responses in nursing and adult rats, *J. Nutr. 116*, 1965−1976.
22. Jones, D. P., Miller, L. A., and Chesney, R. W. (1993) Polarity of taurine transport in cultured renal epithelial cell lines: LLC-PK_1 and MDCK, *Am. J. Physiol. 265*, F137−F145.
23. Uchida, S., Nakanishi, T., Moo Kwon, H., Preston, A. S., and Handler, J. S. (1991) Taurine behaves as an osmolyte in Madin-Darby canine kidney cells, *J. Clin. Invest. 88*, 656−662.
24. Jones, D. P., Miller, L. A., and Chesney, R. W. (1995) The relative roles of external taurine concentration and medium osmolality in the regulation of taurine transport in LLC-PK_1 and MDCK cells, *Pediatr. Res. 37*, 227−232.

BI701979H